Spectroscopic Properties of Mg−Chlorin, Mg−Bacteriochlorin, and Bacteriochlorophylls *a*, *b*, *c*, *d*, *e*, *f*, *g*, and *h* Studied by Semiempirical and Ab Initio MO/CI Methods

Juha Linnanto* and Jouko Korppi-Tommola

Department of Chemistry, University of Jyväskylä, P.O.Box 35, FIN-40351 Jyväskylä, Finland

Received: June 15, 2000; In Final Form: November 16, 2000

The semiempirical PM3 method has been used to calculate fully optimized structures of bacteriochlorophylls *a*, *b*, *c*, *d*, *e*, *f*, *g*, and *h*, magnesium−chlorin, and magnesium−bacteriochlorin. Several configuration interaction (CI) methods, the PM3 (5,5) CIS and CISD, ZINDO/S CIS (n,n) with $2 < n < 30$, and ab initio CIS (5,5)/6-31G* methods, were tested for their predictive power in estimation of spectroscopic properties of bacteriochlorophylls. The ZINDO/S CIS (15,15) method turned out the best results for overall simulation of absorption spectra. Both the transition energies and relative intensities of the Q_y, Q_x, and Soret bands were correctly predicted. The effect of solvent coordination on the transition energies and oscillator strengths was also studied. The calculations predict solvent-induced spectroscopic shifts of the Q_x and Soret bands, whereas the Q_y transitions remain practically unshifted, in accord with experimental findings. The shifts are due to solvent-induced energy level shifts and charge redistribution of the magnesium atom in the excited states of bacteriochlorophylls. The results are discussed with reference to spectroscopic properties of bacteriochlorophylls in solution, in aggregates, and in photosynthetic light harvesting antenna.

1. Introduction

Bacteriochlorophylls are pigments that Nature has developed for the use of bacterial photosynthesis, which became functional more than 3 billion years ago. One of the most striking features of photosynthetic bacteria (green and purple bacteria) is their ability to fix carbon under unoxygenic conditions, a necessary condition of evolution of life under circumstances, when an oxygen atmosphere was not present. Evolution of the phototropic bacteria has been a necessary step for development of more advanced bacterial species, algae and plants, that release oxygen in the atmosphere for the use of life forms consuming oxygen to produce energy.[1]

Photosynthetic bacteria contain a variety of bacteriochlorophylls as compared to only two major pigments, chlorophyll *a* and *b* (Chl *a* and Chl *b*), present in algae and plants.[2] Bacteriochlorophylls (Bchl) may be divided into two groups, to bacteriochlorins (Bchl *a*, Bchl *b*, Bchl *g*, and Bchl *h*) and chlorins (Bchl *c*, Bchl *d*, Bchl *e*, and Bchl *f*) according to their structural properties (Figure 1 and Table 1). In the former group, both B (II) and D (IV) rings are partly saturated. Their Q_y absorption maxima in monomeric solutions are found around 775 nm. The latter group of bacteriochlorophylls contain only one reduced pyrrole ring like Chl *a* and Chl *b*, and their Q_y absorption maxima are observed around 660 nm. Bacteriochlorophylls may be distinguished by the substitutions at C8 and C12 positions and by the esterifying alcohol at C17.[3] Additionally, stereochemistry at the C3[1] (R or S) position may vary from compound to compound. Six esterifying alcohols at the C17[3] position have been identified; the most common alcohols being phytol and farnesol.

Bchl *a* is the most widely distributed pigment found in photosynthetic bacteria. Bchl *a* is present in purple, green filamentous, and green sulfur bacteria. In purple bacteria, it is functional in both light harvesting antenna proteins as well as in the reaction center. Bchl *a* is also the pigment of the base plate and the reaction center of green sulfur bacteria.[1] Bchl *b* is found in purple bacteria like *Rhodopseudomonas* (*Rbs.*) *viridis*, *Rbs. sulfoviridis*, *Thiocapsa pfennigii*, *Ectothiorhodospira* (*Ec.*)-*halochloris*, and *Ec. abdelmaleki*.[3] Bchl *b* contains an ethylidene group at the C8 position as compared to an ethyl group in Bchl *a*. The most common C17[3] substituents in Bchl *a* and Bchl *b* are the phytol and geranylgeraniol groups. Bchl *g* is the main pigment in heliobacteria.[4] Because Bchl *g* contains a vinyl group in position C3 and an ethylidene group at C8, it has structural resemblance to Chl *a* and Bchl *b*, respectively. The esterifying alcohol is a farnesyl chain. Bchl *g* is functional in PSI-type RC connected to a small antenna complex located in the cytoplasmic membrane of heliobacteria. Bchl *h*, which is an as-yet undiscovered compound, is a hypothetical vinyl-substituted analogue

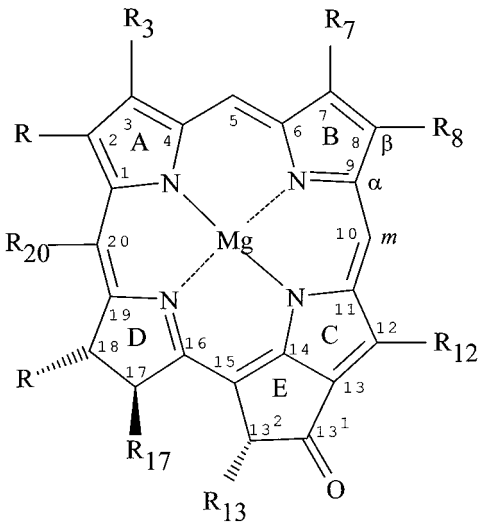

Figure 1. Molecular structure of bacteriochlorophylls. For substituents R_i of individual bacteriochlorophylls, see Table 1.

* To whom correspondence should be addressed.

10.1021/jp0021547 CCC: $20.00
Published on Web 03/22/2001

TABLE 1: Description of Substituents of Individual Bacteriochlorophylls, Mg−chlorin, and Mg−bacteriochlorin (for Basic Structure See Figure 1)

molecule	R_3	R_7	R_8	R_{12}	R_{13}	R_{17}	R_{20}	7,8-bond
Mg−C[a]	−H	−H	−H	−H		−H	−H	doublet
Mg−BC[a]	−H	−H	−H	−H		−H	−H	singlet
Bchl *a*[b]	−CO−CH_3	−CH_3	−C_2H_5	−CH_3	−CO−O−CH_3	−C_2H_4−CO−O−R′[c]	−H	singlet
Bchl *b*[b]	−CO−CH_3	−CH_3	=CH−CH_3	−CH_3	−CO−O−CH_3	−C_2H_4−CO−O−R′[c]	−H	singlet
Bchl *c*[b]	−CHOH−CH_3	−CH_3	−C_2H_5	−CH_3	−H	−C_2H_4−CO−O−R′[d]	−CH_3	doublet
			−C_3H_7	−C_2H_5				
			−C_4H_9					
Bchl *d*[b]	−CHOH−CH_3	−CH_3	−C_2H_5	−CH_3	−H	−C_2H_4−CO−O−R′[d]	−H	doublet
			−C_3H_7	−C_2H_5				
			−C_4H_9					
Bchl *e*[b]	−CHOH−CH_3	−CHO	−C_2H_5	−C_2H_5	−H	−C_2H_4−CO−O−R′[d]	−CH_3	doublet
			−C_3H_7					
			−C_4H_9					
Bchl *f*[b]	−CHOH−CH_3	−CHO	−C_2H_5	−C_2H_5	−H	−C_2H_4−CO−O−R′[d]	−H	doublet
Bchl *g*[b]	−CH=CH_2	−CH_3	=CH−CH_3	−CH_3	−CO−O−CH_3	−C_2H_4−CO−O−R′[d]	−H	singlet
Bchl *h*[b]	−CH=CH_2	−CH_3	−C_2H_5	−CH_3	−CO−O−CH_3	−C_2H_4−CO−O−R′[d]	−H	singlet

[a] Without ring E and R is H. [b] R is CH_3. [c] R′ is phytyl. [d] R′ is farnesyl.

of Bchl *a*. Bchl *h* contains a vinyl group in position C3 like Bchl *g* but an ethyl group at C8 and differs in this respect from Bchl *g*.[5]

Bchls *c*, *d*, and *e*, that may have several homologous structures, are the most abundant pigments in green sulfur and green filamentous bacteria. The pigments are located in vesicles called chlorosomes that are attached to the internal surface of the cytoplasmic membrane via a base plate. Chlorosomes are built from stacked tube like structures each containing of the order of 10000 pigments, and they function as light harvesting antenna in these bacteria. Excluding stereochemistry (*R* or *S* configuration) at C3[1], different homologues of Bchls *c*:s, Bchls *d*:s, and Bchls *e*:s differ by substituents at C8, C12, and C17[3]. In most cases, the esterifying alcohol is farnesol or stearol. The substituent at C12 is either ethyl or methyl in Bchl *c* and *d*, whereas only the ethyl substituents have been found for Bchl *e*. Bchl *c* and Bchl *e* may be distinguished from Bchl *d* by an additional methyl group at C20. Bchl *e* has the meso methyl group and an aldehyde group at C7. Bchl *f* differs from Bchl *e* with respect to the substituent at C20, the former having no methyl group at this location.[2]

An abundance of structural data is available for chlorophylls and chlorins as isolated molecules.[6−10] Crystal structures of bacteriopheophorphides[11,12] and bacteriochlorins[13,14] have been published. Structures of molecular assemblies containing Bchl *a* or *b* in a few photosynthetic bacteria have been resolved. The circular arrangement of the pigments in the LH1 light harvesting antenna of *Rps. viridis* containing Bchl *b* was resolved by electron microscopy.[15] Detailed atomic structures of Bchl *a*'s embedded in a membrane protein have been determined for the reaction centers (RC) of purple bacteria *Rps. viridis*[16] and *Rhodobacter* (*Rh.*) *sphaeroides*.[17] The atomic coordinates of the LH2 antenna protein complexes of *Rps. acidophila*[18] and *Rhodospirillum* (*Rs.*) *molischianum*[19] that also contain Bchl *a* have became available recently. The experimental structural data of bacteriochlorophylls serve as reference for testing the computational methods used in the present study.

There is abundant experimental data on spectroscopic properties of bacteriochlorophylls.[20] One of the earliest spectroscopic studies of porphyrins was carried out by Miller et al.[21] Recently there has been a renewed interest in spectroscopy of porphyrins related to bacterial photosynthesis. Ground-state spectroscopy of bacteriochlorophylls has been studied in solution, [22,23] in rigid matrixes,[24] and in a protein environment.[25] The Raman spectrum of Bchl *a* in the S_1 state has been published.[26] Site-selective low-temperature spectroscopic data for free-base bacteriochlorin has become available.[27] Spectroscopic properties of Bchl *c*[28] have been studied extensively because they can be relatively easily isolated from chlorosomes of green sulfur bacteria. Bchl *c* in chlorosomes shows reversible aggregation−deaggregation under hexanol treatment. Several homologues of Bchl *c* and Bchl *d* have been isolated.[29−31]

Because Bchls *a*, *b*, and *g* belong structurally to bacteriochlorins, they share common features in their absorption spectra. The Q_y bands of these compounds are located at 772.6 nm (acetone), 796.2 nm (diethyl ether), and 767.2 nm (acetone).[32] Additionally the Q_x bands of Bchls *a*, *b* and *g*, located at 583.3, 578.8, and 564.5 nm, respectively, are nicely separated from the Q_y bands and can be identified reliably. Bchl *a* has the most blue shifted Soret band and broadest line widths. The Q_y absorption bands of Bchl *c*, *d* and *e* are found at 667.2, 656.1, and 648.9 nm in acetone, respectively.[32,33] The absorption spectrum of Bchl *c* is slightly red shifted with respect to the spectrum of Bchl *d*, otherwise the spectra are quite similar.[23] The spectrum of Bchl *e* shows an exceptionally red shifted Soret band absorbing at about 461.6 nm as compared to 435.7 and 431.2 nm in Bchl *c* and *d*, respectively. The Q_y band of Bchl *e* has much lower intensity than the corresponding bands of Bchl *c* and *d*.[34]

Knowing excited states of bacteriochlorophylls is fundamental for understanding their properties in various environments, in solution, in self-assembled aggregates, and in photosynthetic light harvesting antenna. It is the purpose of the present study to try to predict the spectroscopic characteristics of each bacteriochlorophyll by using a single systematic computational approach. We hope to answer questions like why the Q_y transition energies of bacteriochlorins are much more red shifted than those of chlorins, why the Q_x and Soret bands of Bchl *e* are much more red shifted than the corresponding bands in Bchl *c* and Bchl *d*, or why solvent-induced shifts are observed for the Q_x and Soret bands of bacteriochlorophylls, whereas the position of the Q_y band is almost unshifted.[22] Environmental effects are present also in the photosynthetic light harvesting antenna. In the bacterial LH2 antenna of *Rps. acidophila*, the structure of which is known to atomic detail, Bchl *a*−nearby amino acid interactions account for most of the observed spectral shift of the B800-ring of the antenna.[35] Additionally, the pigments in the B850 ring showed orbital overlap interactions that could not be explained by the dipole−dipole interaction.[35] Such interactions also effect energy transfer rates in aggregated chromophore complexes.[36] The role of the amino acids in the

TABLE 2: Calculated Heavy Atom Distances in Mg-chlorin, Mg-bacteriochlorin and the Bacteriochlorophylls

distance[a]	Mg−C	Mg−BC	Bchl *a*	Bchl *b*	Bchl *c*	Bchl *d*	Bchl *e*	Bchl *f*	Bchl *g*	Bchl *h*
1−2	1.465	1.472	1.423	1.484	1.477	1.468	1.478	1.469	1.477	1.428
2−3	1.355	1.348	1.407	1.364	1.372	1.370	1.371	1.370	1.370	1.402
3−4	1.467	1.485	1.438	1.478	1.467	1.474	1.469	1.476	1.483	1.439
4−5	1.367	1.387	1.432	1.353	1.360	1.359	1.358	1.357	1.351	1.420
5−6	1.406	1.386	1.354	1.443	1.426	1.432	1.431	1.435	1.444	1.361
6−7	1.436	1.513	1.517	1.526	1.452	1.454	1.453	1.453	1.523	1.518
7−8	1.384	1.537	1.548	1.509	1.381	1.380	1.389	1.388	1.515	1.548
8−9	1.436	1.506	1.517	1.471	1.448	1.450	1.441	1.443	1.469	1.517
9−10	1.406	1.346	1.446	1.363	1.400	1.396	1.406	1.404	1.362	1.441
10−11	1.367	1.429	1.355	1.424	1.384	1.389	1.379	1.383	1.425	1.357
11−12	1.467	1.427	1.495	1.430	1.463	1.460	1.467	1.465	1.429	1.492
12−13	1.355	1.386	1.363	1.407	1.385	1.388	1.382	1.384	1.408	1.364
13−14	1.465	1.420	1.475	1.428	1.450	1.447	1.452	1.451	1.430	1.474
14−15	1.403	1.423	1.388	1.430	1.417	1.422	1.417	1.422	1.432	1.390
15−16	1.372	1.347	1.402	1.357	1.365	1.364	1.366	1.365	1.357	1.399
16−17	1.506	1.505	1.527	1.523	1.520	1.524	1.520	1.524	1.521	1.526
17−18	1.533	1.532	1.557	1.556	1.553	1.558	1.553	1.558	1.556	1.557
18−19	1.506	1.507	1.516	1.521	1.525	1.519	1.525	1.518	1.521	1.516
19−20	1.372	1.427	1.356	1.374	1.371	1.361	1.371	1.360	1.374	1.356
20−1	1.403	1.352	1.430	1.420	1.455	1.434	1.455	1.435	1.420	1.430
NA-1	1.389	1.459	1.400	1.354	1.353	1.348	1.352	1.347	1.355	1.390
NA-4	1.434	1.377	1.380	1.445	1.450	1.451	1.451	1.452	1.448	1.394
NB-6	1.383	1.347	1.438	1.330	1.369	1.368	1.366	1.367	1.328	1.428
NB-9	1.383	1.417	1.336	1.453	1.417	1.421	1.419	1.421	1.460	1.340
NC-11	1.434	1.398	1.445	1.418	1.440	1.436	1.443	1.440	1.415	1.445
NC-14	1.389	1.414	1.353	1.356	1.339	1.341	1.337	1.339	1.354	1.352
ND-16	1.387	1.435	1.346	1.403	1.386	1.388	1.385	1.387	1.405	1.348
ND-19	1.387	1.332	1.431	1.388	1.413	1.405	1.414	1.407	1.387	1.427
Mg−NA	1.887	1.881	2.325	2.372	2.393	2.377	2.391	2.375	2.366	2.331
Mg−NB	1.841	1.837	2.467	2.454	2.424	2.426	2.427	2.428	2.459	2.463
Mg−NC	1.887	1.885	1.830	1.832	1.841	1.837	1.840	1.836	1.830	1.830
Mg−ND	2.466	2.505	1.829	1.821	1.819	1.817	1.820	1.817	1.820	1.827
A, B, C, Mg	0.000	0.005	0.096	0.134	0.059	0.088	0.048	0.077	0.107	0.076
NA-NB	2.858	2.889	3.052	3.026	3.078	3.005	3.081	3.006	3.040	3.047
NA-NC	3.716	3.697	4.067	4.116	4.148	4.123	4.148	4.122	4.114	4.073
NA-ND	2.831	2.801	2.928	2.893	2.869	2.916	2.866	2.918	2.914	2.947
NB−NC	2.858	2.849	2.732	2.769	2.703	2.739	2.708	2.745	2.774	2.735
NB−ND	4.307	4.341	4.268	4.226	4.202	4.202	4.205	4.205	4.240	4.266
NC−ND	2.831	2.865	3.074	3.106	3.144	3.108	3.143	3.103	3.084	3.063

[a] The PM3 CI method was used for full geometry optimization. Experimental values may be found in refs 6−14. [b] 1 is C1; NA is nitrogen in ring A; A, B, C, Mg is the distance between plane NA−NB−NC and the Mg atom.

LH2 antenna of *Rs. molischianum* is even stronger. It seems that chromophore−chromophore or chromophore−protein interactions have to be estimated by using quantum chemical methods to obtain feasible interaction energies. To evaluate these reliable computational methods, estimation of electronic properties of monomeric chromophores are needed.

Because bacteriochlorophylls are large atomic systems, computational limits become soon a restricting factor in predicting molecular properties of these compounds by quantum chemical methods. The computational possibilities have improved to allow ab initio level calculations on bacteriochlorin,[37,38] bacteriopheophorbide,[39,40] bacteriopheophytin,[41] and Bchl *a*.[39,41] Electrochromic effects of charge separation of the pigments in the reaction center of *Rps. viridis* containing Bchl *b* have been studied at the INDO level of calculation.[42] In the present work, semiempirical and ab initio quantum chemical methods with configuration interaction are used to compute structures and electronic states of bacteriochlorophylls and to predict their absorption spectra in a vacuum. The effects of solvent coordination on excited-state energies and on absorption spectra of the bacteriochlorophylls will be studied. In forthcoming papers, further results from ab initio and density functional calculations will be given. For a review of quantum chemical calculations on porphyrin type compounds, we refer to our recent work on calculations of structures, electronic states, and spectra of chlorophylls *a*, *b*, c_1, c_2, c_3, and *d*.[43]

2. Computational Methods

The monomer structures of bacteriochlorophylls *a*, *b*, *c*, *d*, *e*, *f*, *g*, and *h* with all homologous structures (Figure 1 and Table 1), magnesium-bacteriochlorin (Mg−bacteriochlorin, Mg−BC), and magnesium−chlorin (Mg−chlorin, Mg−C) were fully optimized at the semiempirical PM3[44] level on a Silicon Graphics O2 and Indigo2 workstations by using SPARTAN[45] (Version 5.0) software. Geometry optimization was then continued on a Cray C94 supercomputer at the National Centre for Scientific Computing (CSC) in Espoo, Finland, at the PM3/CI level by using the MOPAC[46] (version 6.0) software package. Optimized monomer geometry was used in calculation of atomic charges, transition energies, and oscillation strengths. Atomic charges were calculated at the semiempirical PM3 level and ab initio Hartree−Fock level by using the basis set 6-31G* on a Silicon Graphics Indigo2 workstation. Geometry optimization of the 1:1 complexes of the Bchls and acetone were done at PM3 level by using the AlphaServer ES-40 workstation. In this case, only one homologous structure per Bchl was studied, in Bchl *c* and *d* the substituents at R_8 and at R_{12} positions were ethyl and methyl groups, respectively; in Bchl *e*, ethyl groups were inserted at R_8 and at R_{12} positions. Transition energies and oscillation strengths were calculated at ZINDO/S CIS (15,15) or (20,20)[47−49] level by using the HyperChem[50] (version 5.0) software running on a pentium PC. PM3 CIS (5,5) and

CISD (5,5) level calculations were carried out by using the SPARTAN software on a Silicon Graphics O2 workstation and at ab initio CIS (5,5)/6-31G* level by using the Gaussian94[51] software on a Silicon Graphics Indigo2 workstation. The calculated transition energies were correlated to experimental transition energies by using linear least-squares fits. Experimental Q_y, Q_x, and Soret transition energies of bacteriochlorophylls were taken as absorption wavelengths of monomeric bacteriochlorophylls in inert solutions.

3. Results

3.1. Structure of Bacteriochlorophylls. A typical feature of geometry optimized structures of all bacteriochlorophylls obtained by using the semiempirical PM3 Hamiltonian was that the Mg atom of the porphyrins is neither centered nor located in the plane of the porphyrin ring. The most important computed distances and bond angles of bacteriochlorophylls and Mg−bacteriochlorin and Mg−chlorin are given in Table 2. In the experimental structures, the magnesium atom is at the center of the planar porphyrin ring.[6−10,14] For the model compounds Mg−bacteriochlorin and Mg−chlorin, almost planar structures with Mg−atom in the porphyrin plane, but the Mg atom shifted about 0.6 Å toward the B ring, were obtained. We think that poor PM3 parametrization of the magnesium atom of the software used is the reason for the asymmetric positioning of the central atom in these molecules. Similar trends at the PM3 level of calculation was observed for chlorophylls.[43]

The main difference between Mg−bacteriochlorins and Mg−chlorins is localization of electrons in the B ring. In Mg−bacteriochlorins, the bond length between the C_7 and C_8 atoms is about 0.12 Å longer than the corresponding bond length in Mg−chlorins (see Table 2). The difference is related to the type of bonding of the C_7 and C_8 atoms, in bacteriochlorins a single bond and in chlorins a double bond connects these atoms. These characteristics are well reproduced in the PM3 optimizations. Calculated bond lengths of the Mg−bacteriochlorin and Mg−chlorin are not much different from the corresponding bond lengths in the corresponding bacteriochlorophylls (Table 2).

At PM3 minimum energy in a vacuum the esterifying alcohol tails of Bchls at R_{17} are twisted above the porphyrin plane. The calculated energy difference (PM3, heats of formation) between the two structures, where the hydrocarbon tail is bent above the porphyrin plane and where it is directed away from the center and parallel to the porphyrin plane, is about 20 kJ mol^{-1}. Solvent coordination to the magnesium atom induces straightening of the hydrocarbon tail.

3.2. Energy Levels and Molecular Orbitals. *3.2.1. Energy Levels at Minimum PM3 Geometry*. Energy levels of the 20 highest occupied and 20 lowest unoccupied molecular orbitals calculated for PM3 minimum energy geometry are shown in Figure 2. A common feature of the molecular orbital energies in all bacteriochlorophylls studied and in Mg−chlorin and in Mg−bacteriochlorin is that the two highest occupied and two lowest unoccupied molecular orbitals are well separated from the rest of the energy levels. The molecular orbital energy difference of the LUMO + 1 and LUMO levels in Mg−bacteriochlorins is about 1 eV, whereas the corresponding difference in Mg−chlorins is only about 0.5 eV. Similar behavior is observed for the HOMO and HOMO − 1 orbitals. The molecular orbital energy difference of the HOMO and LUMO levels in bacteriochlorins is smaller than the corresponding difference in chlorins, which explains the fairly large difference in Q_y transition energies of the two chromophore groups. It is concluded that the structural differences between

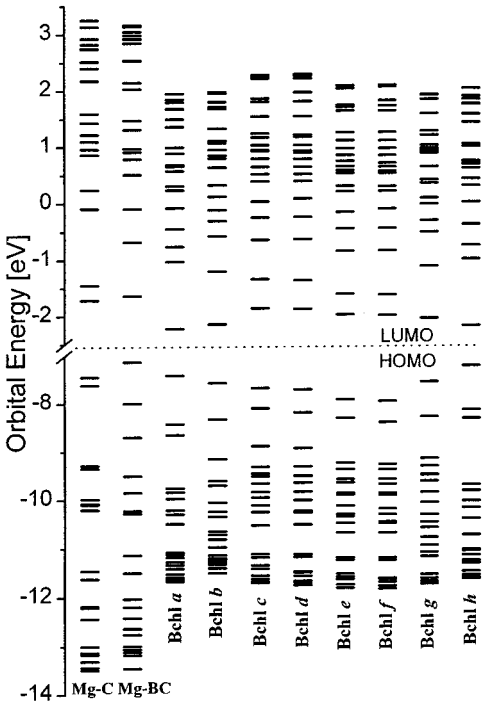

Figure 2. Molecular orbital energies of the Mg−chlorin, Mg−bacteriochlorin, and bacteriochlorophylls *a*, *b*, *c*, *d*, *e*, *f*, *g*, and *h*. The states below the dashed line are occupied, whereas those above are unoccupied. Abbreviations below each energy level column refer to the compound in question.

Mg−bacteriochlorin type and Mg−chlorin type bacteriochlorophylls, respectively, are reflected in electronic energies and to the most important spectroscopic transitions of these compounds. Each Bchl is expected then to have a characteristic absorption spectrum.

3.2.2. Molecular Orbitals of Bchl a, Bchl b, Bchl g, and Bchl h. Spatial PM3 contour maps of three lowest unoccupied and three highest occupied molecular orbitals of Bchl *g* and Bchl *e* are shown in Figure 3 as representative examples of spectroscopically relevant molecular orbitals of bacteriochlorin and chlorin type Bchls, respectively. In bacteriochlorins, the LCAO coefficients of unoccupied molecular orbitals from LUMO + 1 to LUMO + 4 are quite similar. A notable feature is that in Bchl *a*, Bchl *b*, and Bchl *g* the LUMO + 2, LUMO + 1, and HOMO − 1 states contain high electron density on the central magnesium atom. Molecular orbitals of Bchl *h* are almost similar with the exception that also the HOMO − 2 state contains high electron density on the central magnesium atom.

The orbital shapes of Bchl *a* and Bchl *h* are very similar. In Bchl *a* and Bchl *h*, the HOMOs are located mostly in the A ring. In Bchl *a*, the electron density of the LUMO orbital is located on the C and E rings. In Bchl *b* and Bchl *g*, the HOMOs are spread over the E and C rings, whereas the LUMO densities are distributed almost entirely over the A ring. There is practically no electron density on the central magnesium in the HOMO and LUMO orbitals of bacteriochlorins. In Bchl *a* and Bchl *b*, the HOMO − 1 orbital is spread quite evenly over the entire porphyrin plane. The HOMO − 2 orbitals of Bchl *b* and Bchl *g* are near the C ring, whereas the corresponding orbital of Bchl *a* is around the A ring. The HOMO − 3 orbital of Bchl *g* is almost entirely localized *on the farnesyl tail* showing typical π-electron distribution.

3.2.3. Molecular Orbitals of Bchl c, Bchl d, Bchl e, and Bchl f. Figure 3 shows six molecular orbital contours of Bchl *e* from HOMO − 2 to LUMO + 2. The MOs of Mg−chlorins, Bchl *c*,

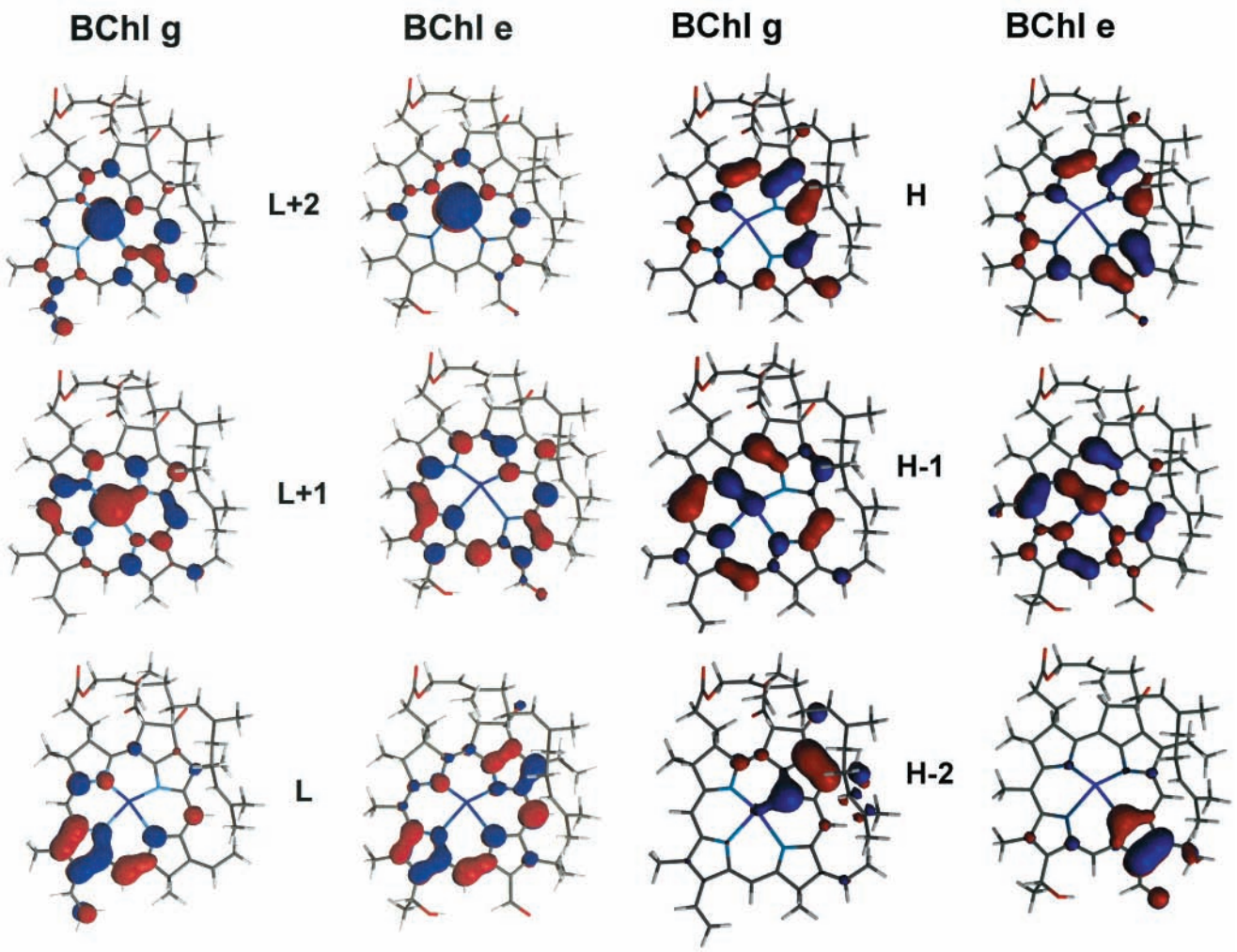

Figure 3. (a) Selected molecular orbitals of Bchl *g* (left) and Bchl *e* (right). From top to bottom, LUMO + 2 (L + 2), LUMO + 1 (L + 1), and LUMO (L) orbitals. (b) Selected molecular orbitals of Bchl *g* (left) and Bchl *e* (right). From top to bottom, HOMO (H), HOMO − 1 (H − 1), and HOMO − 2 (H − 2) orbitals.

Bchl *d*, and Bchl *f*, are very similar to those of Bchl *e*. The LUMO + 2 and the HOMO − 1 states have considerable electron density localized on the magnesium atom. Bchl *c* and *d* have in addition small electron density on the magnesium atom in the LUMO + 1 state. The LUMO + 1 states of Bchl *c*, Bchl *d*, Bchl *e*, and Bchl *f* show electron density that is distributed over the outer ring carbons of the porphyrin in contrast to high electron density observed on the magnesium atom of the LUMO + 1 in bacteriochlorins. The LUMO electron density of the chlorins is spread over the A and C rings, whereas the HOMO orbital covers the B and C rings. The HOMO − 2 state is localized on the B ring. The HOMO − 3 and HOMO − 4 states of Bchl *e* and *f* and HOMO − 3 state of Bchl *c* and *d* consist of *π-type orbitals that are localized on the farnesyl tail*. This suggests that the farnesyl group may play a role in spectroscopy of chlorins in the Soret region. Further details on molecular orbitals of Bchls may be obtained from the authors on request.

3.3. CI Description of the Excited States. *3.3.1. Energy Levels and CI Space*. For proper describtion of the excited states of bacteriochlorophylls, electron correlations have to be included in the calculations. Several limited CI calculations at ZINDO/S, PM3, and ab initio (6-31G* basis set) levels were performed to test the predictive power of each method. Bacteriochlorophyll *a* was used as an example. Excited-state energy levels are dependent on the type of MOs chosen in the CI expansion and on the extent of the CI space used in the calculation. We used the ZINDO/S CIS method to study the size effects of the CI space from (2,2) up to (15,15) expansions. The computed Q_y, Q_x, and Soret transition energies of Bchl *a* converged toward the experimental energies as the size of the CI space was increased up to (15,15).[43] Expanding the single excitation CI space to (25,35) did not improve the results in practical terms. Including both single and double excitations in a PM3 CISD (5,5) calculation gave results that are closest to the experimental Q_y, Q_x, and Soret transition energies. The ab initio CIS (5,5)/6-31G* calculation clearly overestimates the transition energies of the three lowest excited states of bacteriochlorophylls.

3.3.2. CIS and CISD Wave Functions. Tables 3−6 show the main configurations (weight ≥ 5%) of the Q_y, Q_x, and *B* (Soret) transitions of all bacteriochlorophylls studied as well as those for Mg−bacteriochlorin and Mg−chlorin. Tables 3 (bacteriochlorins) and 4 (chlorins) give the most important configurations for single excitations at (5,5) truncation with PM3 orbitals. Tables 5 (bacteriochlorins) and 6 (chlorins) show the corresponding results when both single and double excitations were included in the calculation (PM3 CISD (5,5)).

The CIS calculations with PM3 wave functions of the minimum energy structures of bacteriochlorophylls show that the Q_y state of bacteriochlorins contain two major configurations, HOMO − 1 → LUMO (H − 1 → L) and HOMO → LUMO +

TABLE 3: Excited States of Mg−Bacteriochlorin and Bacteriochlorophylls Bchl *a*, Bchl *b*, Bchl *g*, and Bchl *h* at PM3 Minimum Energy Obtained with the PM3 CIS (5,5) Method

state	main configuration (C ≥ |0.05|)
Mg−BC Q_y	−0.06(H-4→L+3) − 0.05(H-3→L+1) + 0.06(H-2→L+3) - **0.32(H-1→L+1)**
	−0.11(H-1→L+2) − **0.61(H→L)** + 0.05(H→L+4)
Q_x	−0.13(H-3→L) − 0.08(H-2→L+1) + 0.10(H-2→L+2) + **0.61(H-1→L)** − **0.30(H→L+1)**
B	−0.05(H-4→L+1) − 0.09(H-3→L) − 0.07(H-2→L) + 0.11(H-1→L+1)
	0.07(H-1→L+2) − 0.19(H→L+1) − **0.65(H→L+2)** + 0.05(H→L+3)
Bchl *a* Q_y	−**0.51(H-1→L)** + 0.10(H-1→L+1) − 0.08(H-1→L+3) + 0.22(H→L)
	0.27(H→L+1) − **0.30(H→L+2)** + 0.11(H→L+3)
Q_x	−0.05(H-3→L) + 0.05(H-3→L+3) + 0.05(H-2→L+1) − 0.18(H-1→L) − 0.13(H-1→L+1)
	−**0.64(H→L)** + 0.12(H→L+1) − 0.12(H→L+2) − 0.08(H→L+3)
B	0.06(H-3→L) − 0.12(H-1→L+1) − 0.08(H-1→L+2) − **0.44(H→L+1)** − **0.52(H→L+2)**
Bchl *b* Q_y	0.07(H-3→L) − 0.06(H-2→L) − **0.48(H-1→L)** + 0.15(H-1→L+1)
	−0.09(H-1→L+3) + 0.22(H→L) + **0.40(H→L+1)** − 0.15(H→L+2)
Q_x	0.05(H-3→L) + 0.05(H-3→L+1) + 0.05(H-2→L+1) − 0.21(H-1→L)
	−0.10(H-1→L+1) − **0.64(H→L)** + 0.14(H→L+1) − 0.08(H→L+3)
B	−0.05(H-3→L+2) − 0.05(H-3→L+3) − 0.05(H-2→L+2) − 0.12(H-1→L) − 0.19(H-1→L+1)
	−0.09(H-1→L+2) − **0.28(H→L+1)** − **0.57(H→L+2)** - 0.13(H→L+3)
Bchl *g* Q_y	0.09(H-4→L) − **0.50(H-1→L)** − 0.13(H-1→L+1) + 0.07(H-1→L+2)
	−0.09(H-1→L+3) − 0.14(H→L) + **0.42(H→L+1)** + 0.14(H→L+2)
Q_x	0.14(H-4→L) + 0.05(H-2→L+1) − 0.17(H-1→L) + 0.10(H-1→L+1)
	0.65(H→L) + 0.05(H→L+1) − 0.08(H→L+2) + 0.08(H→L+3)
B	0.05(H-2→L+2) + 0.05(H-2→L+3) + **0.29(H-1→L)** + **0.28(H-1→L+1)** − 0.08(H-1→L+2)
	−0.07(H-1→L+3) + **0.23(H→L)** + **0.29(H→L+1)** + **0.31(H→L+2)** + 0.15(H→L+3)
Bchl *h* Q_y	−**0.40(H-2→L)** − 0.13(H-2→L+1) + 0.07(H-2→L+3) + 0.08(H-1→L)
	0.66(H-1→L+1) − **0.41(H→L)** + 0.26(H→L+1) + 0.27(H→L+2) + 0.09(H→L+3)
Q_x	−0.31(H-2→L) + 0.10(H-2→L+1) − 0.05(H-2→L+3) + 0.08(H-1→L)
	0.54(H→L) + **0.27(H→L+1)** + 0.14(H→L+2) − 0.06(H→L+3)
B	0.10(H-3→L) −0.07(H-2→L) − 0.10(H-2→L+1) + **0.20(H-2→L+2)**
	0.06(H-1→L+1) − 0.05(H→L) + **0.32(H→L+1)** − **0.52(H→L+2)**

TABLE 4: Excited States of Mg−Chlorin and Bacteriochlorophylls Bchl *c*, Bchl *d*, Bchl *e*, and Bchl *f* at PM3 Minimum Energy Obtained with the PM3 CIS (5,5) Method

state	main configuration (C ≥ |0.05|)
Mg−C Q_y	0.47(H-1→L+1) + 0.10(H-1→L+3) + **0.52(H→L)**
Q_x	0.08(H-4→L) − 0.09(H-3→L+3) + **0.52(H-1→L)** + 0.08(H-1→L+2) − **0.45(H→L+1)**
B	−0.10(H-4→L+1) − 0.29(H-3→L) − 0.12(H-3→L+2)
	−**0.36(H-1→L+1)** + **0.36(H→L)** + **0.36(H→L+2)**
Bchl *c* Q_y	−0.16(H-1→L) − **0.33(H-1→L+1)** + 0.10(H-1→L+3) + **0.56(H→L)**
	−0.14(H→L+1) − 0.08(H→L+2) + 0.06(H→L+3)
Q_x	−0.08(H-4→L) − 0.06(H-4→L+3) + 0.06(H-2→L) + 0.47(H-1→L) − 0.07(H-1→L+1)
	0.13(H-1→L+2) + 0.20(H→L) + **0.44(H→L+1)** + 0.10(H→L+2) − 0.06(H→L+3)
B	−0.07(H-4→L) − 0.07(H-4→L+1) − 0.15(H-2→L) + 0.06(H-1→L) + **0.25(H-1→L+1)**
	−**0.31(H-1→L+2)** + 0.12(H→L) + 0.13(H→L+1) − **0.51(H→L+2)** + 0.05(H→L+3)
Bchl *d* Q_y	0.18(H-1→L) + **0.33(H-1→L+1)** + 0.09(H-1→L+3) + **0.55(H→L)**
	−0.17(H→L+1) − 0.09(H→L+2) − 0.05(H→L+3)
Q_x	−0.06(H-4→L) + 0.05(H-4→L+3) + 0.05(H-2→L) − **0.44(H-1→L)** + 0.09(H-1→L+1)
	−0.13(H-1→L+2) + 0.24(H→L) + **0.45(H→L+1)** + 0.08(H→L+2) + 0.07(H→L+3)
B	−0.05(H-4→L) − 0.17(H-2→L) − 0.24(H-1→L+1) + **0.30(H-1→L+2)**
	0.12(H→L) + 0.14(H→L+1) − **0.53(H→L+2)** - 0.05(H→L+3)
Bchl *e* Q_y	0.05(H-2→L+1) + 0.18(H-1→L) + **0.35(H-1→L+1)** − 0.11(H-1→L+3)
	0.54(H→L) − 0.18(H→L+1) + 0.07(H→L+2) + 0.07(H→L+3)
Q_x	−0.08(H-2→L) + **0.39(H-1→L)** − 0.15(H-1→L+1) − 0.18(H-1→L+2)
	−0.21(H→L) − **0.46(H→L+1)** + 0.16(H→L+2) + 0.07(H→L+3)
B	0.11(H-2→L) + 0.16(H-1→L) + **0.23(H-1→L+1)** + **0.30(H-1→L+2)**
	0.05(H-1→L+4) − 0.21(H→L) − 0.15(H→L+1) − **0.50(H→L+2)**
Bchl *f* Q_y	0.05(H-2→L+1) + 0.18(H-1→L) + **0.35(H-1→L+1)** + 0.11(H-1→L+3)
	0.54(H→L) − 0.18(H→L+1) + 0.07(H→L+2) − 0.07(H→L+3)
Q_x	0.08(H-2→L) − **0.38(H-1→L)** + 0.15(H-1→L+1) + 0.18(H-1→L+2)
	0.20(H→L) + **0.48(H→L+1)** − 0.13(H→L+2) + 0.07(H→L+3)
B	0.12(H-2→L) + 0.15(H-1→L) + **0.22(H-1→L+1)** + **0.31(H-1→L+2)**
	−0.19(H→L) − 0.15(H→L+1) − **0.51(H→L+2)**

1 (H → L + 1, from here on we use the short notation for the configurations), except Bchl *h*. The Q_y state of Bchl *h* is described by the H → L, H − 1 → L + 1, and H − 2 → L configurations. The Q_x state of the bacteriochlorins Bchl *a*, Bchl *b*, Bchl *g*, and Bchl *h* is described by the H → L configuration, but the *B* state is a superposition of several configurations, where at least H → L + 1 and H → L + 2 contribute (Table 3). In chlorins Bchl *c*, Bchl *d*, Bchl *e*, and Bchl *f* the Q_y state is dominated by the singly excited configurations H → L and H − 1 → L + 1. The Q_x state is mainly described by configurations H → L + 1 and H − 1 → L, and the *B* state is a superposition of many configurations but dominated by the singly excited configuration H → L + 2, as shown in Table 4.

The PM3 CISD (5,5) calculations on the bacteriochlorins suggest that the Q_y transition is mainly described by the configuration H → L in contrast with two major configurations obtained for the single excitation scheme. Because HOMO and

TABLE 5: Excited States of Mg−Bacteriochlorin and Bacteriochlorophylls Bchl *a*, Bchl *b*, Bchl *g*, and Bchl *h* at PM3 Minimum Energy Obtained with the PM3 CISD (5,5) Method

state	main configuration (C ≥ |0.05|)
Mg−BC Q_y	0.18(0) + 0.18(H-1→L+1) + **0.61(H→L)** + 0.14(H-1,H→L,L+1) − 0.06(H-1,H→L,L+2) −0.05(H-1→L,H→L+2) + 0.12(H-1→L+1,H→L) + 0.14(H→L,H→L)
Q_x	0.07(H-2→L) + **0.49(H-1→L)** − **0.45(H→L+1)** + 0.09(H→L+2) + 0.05(H-4→L,H-1→L) −0.06(H-1→L,H-1→L) + 0.07(H-1→L+1,H→L+1) − 0.05(H→L+1,H→L+3)
B	0.05(H-4→L+1) + 0.13(H-2→L) + 0.07(H-1→L+1) − 0.05(H-1→L+2) 0.12(H→L+1) + **0.63(H→L+2)** + 0.05(H-1→L+1,H→L+2) 0.06(H-1→L+2,H→L+2) + 0.08(H-1→L,H→L) − 0.09(H-1,H→L+1,L+2)
Bchl *a* Q_y	−0.08(H-3→L) − 0.07(H-1→L) + 0.05(H-1→L+2) − **0.64(H→L)** + 0.14(H→L+3) −0.05(H-3→L,H→L) + 0.12(H-1,H→L,L+1) − 0.12(H-1,H→L,L+2) −0.09(H-1→L,H→L+1) + 0.09(H→L,H-1→L+1) + 0.07(H→L,H-1→L+2)
Q_x	**0.53(H-1→L)** − 0.05(H-1→L+1) − 0.08(H-1→L+3) − **0.33(H→L+1)** − **0.26(H→L+2)** 0.06(H→L+3) − 0.05(H-3→L, H-1→L) − 0.08(H-1→L,H-1→L)
B	−0.06(H-2→L) − 0.07(H-1→L+1) + 0.05(H-1→L+2) − **0.40(H→L+1)** + **0.53(H→L+2)** 0.09(H-1,H→L+1,L+2) + 0.08(H-1→L+2,H→L+1) + 0.07(H-1→L+2,H→L+2) −0.05(H→L,H→L+2) + 0.06(H→L+2,H→L+2)
Bchl *b* Q_y	−0.14(0) − 0.06(H-1→L) + 0.15(H-1→L+1) + **0.62(H→L)** − 0.05(H→L+2) + 0.05(H→L+3) −0.05(H-1→L,H-1→L) − 0.14(H-1,H→L,L+1) − 0.08(H-1,H→L,L+2) − 0.11(H-1→L,H→L+1) −0.05(H-1→L+2,H→L) − 0.11(H→L,H-1→L+1) − 0.05(H→L,H-1→L+2) − 0.13(H→L,H→L)
Q_x	0.06(H-3→L) + 0.05(H-2→L) + **0.50(H-1→L)** + 0.12(H-1→L+1) − 0.05(H-1→L+2) 0.06(H-1→L+3) 0.06(H→L) − **0.43(H→L+1)** − 0.08(H→L+2) + 0.08(H-1→L,H-1→L)
B	0.18(H-1→L) − 0.16(H-1→L+1) + 0.09(H-1→L+2) + **0.25(H→L+1)** − **0.56(H→L+2)** −0.13(H→L+3) −0.06(H-1,H→L+1,L+2) − 0.06(H-1→L+2,H→L+1) + 0.06(H→L+2,H→L+2)
Bchl *g* Q_y	−0.12(0) − 0.09(H-1→L) + 0.14(H-1→L+1) + **0.62(H→L)** − 0.06(H→L+2) + 0.06(H→L+3) −0.06(H-1→L,H-1→L) − 0.15(H-1,H→L,L+1) − 0.07(H-1,H→L,L+2) −0.05(H-1,H→L,L+3) − 0.05(H-1→L,H→L+1) − 0.10(H→L,H-1→L+1) − 0.12(H→L,H→L)
Q_x	−0.09(H-4→L) + **0.50(H-1→L)** + 0.12(H-1→L+1) − 0.07(H-1→L+2) + 0.06(H-1→L+3) 0.08(H→L) − **0.43(H→L+1)** − 0.08(H→L+2) + 0.07(H-1→L,H-1→L)
B	−0.07(H-4→L) − 0.05(H-2→L+3) + 0.17(H-1→L) − 0.20(H-1→L+1) + 0.10(H-1→L+2) 0.06(H-1→L+3) + **0.25(H→L+1)** − **0.50(H→L+2)** − **0.23(H→L+3)** 0.05(H-1→L+1,H-1→L+1) − 0.05(H-1→L+2,H→L+1) − 0.05(H-1,H→L+1,L+2)
Bchl *h* Q_y	0.18(0) −0.05(H-3→L) + 0.14(H-2→L+1) − 0.07(H-2→L+2) − **0.63(H→L)** + 0.07(H→L+2) −0.11(H-2,H→L,L+1) + 0.09(H-2,H→L,L+2) − 0.08(H-2→L+1,H→L) +0.05(H-2→L+2,H→L) +0.17(H→L,H→L)
Q_x	−0.25(H-2→L) + 0.05(H-1→L+1) + **0.59(H→L+1)** - 0.25(H→L+2) + 0.06(H-2→L,H→L+1) 0.08(H-2→L+1,H→L+1) + 0.06(H-2→L+2,H→L+1)
B	−0.05(H-2→L+1) + 0.05(H-1→L+2) + 0.06(H→L) + **0.32(H→L+1)** + **0.59(H→L+2)** −0.09(H-2,H→L+1,L+2) − 0.07(H-2→L+2,H→L+1) + 0.07(H-2→L+2,H→L+2) 0.05(H-1→L+2,H→L+1) − 0.07(H→L,H→L+2)

LUMO states do not contain contribution from magnesium the transition is less subject to solvent shift. The Q_x state includes H − 1 → L and H → L + 1 configurations, whereas the Soret region is a superposition of many configurations, the most important being H → L + 1 and H → L + 2 (Table 5). In chlorins, the Q_y transition includes H → L and H − 1 → L + 1 configurations, whereas the Q_x contains H − 1 → L and H → L + 1 configurations. The Soret states included H → L + 2, H − 1 → L + 2, and H − 1 → L + 1 configurations (Table 6). Examination of the CI wave functions of all bacteriochlorophylls suggest that both Q_x and Soret transitions contain states that have weight on the magnesium atom and, hence, are subject to solvent-induced spectral shifts.

It may be noted that, though the main components of the CIS and CISD wave functions are almost the same, the CIS and CISD wave functions are not the same.

The coefficients of the single and double excitation expansions are different, and hence, the corresponding energies are not the same. Because double (and higher) excitations have an effect on the ground-state energy (Brillouin's theorem),[52] double excitations are reflected in spectroscopic transition energies.

3.4. Absorption spectra of bacteriochlorophylls. *3.4.1. Simulation of Vacuum Spectra.* Table 7 summarizes the estimated and experimental Q_y, Q_x, and *B* transition wavelengths of the bacteriochlorophylls studied. Experimental wavelengths given for the *B* transitions in Table 7 refer to the strongest band component in the Soret region obtained for monomeric solutions.[20] Estimated values were obtained from linear calibrations of experimental and computed (vacuum) energies, as suggested by Petke et al.[53] In Figure 4a, correlations between experimental and ZINDO/S CIS (15,15) Q_y, Q_x, and *B* transition energies of the Bchls studied are shown. Bacteriochlorophyll *a* (black dot) stands out as a distinct case, reflecting structural differences with the other two bacteriochlorins, Bchl *b* and Bchl *g*. Bacteriochlorophylls *c*, *d*, *e*, and *f* (black triangles) including all homologous structures (Table 1) form their characteristic group, and computed Q_y transition energies are the same within few nanometers in these molecules. The computed Q_y and Soret transition energies of Bchl *h* seem to be the most red and blue shifted of all Bchls, respectively. In Figure 4b, correlations at ab initio CIS (5,5)/6-31G* level of computation are shown. Ab initio transition energies seem to be slightly better correlated with the experimental energies than the ZINDO/S results, though the absolute transition energies at the ab initio CIS level were clearly overestimated. The results indicate that the calibration of experimental and computed transition energies is dependent on the computational method used and valid only within a group of molecules with similar structures.

To simulate the UV−visible absorption spectra of the bacteriochlrophylls, the ZINDO/S CIS (15,15) method was used. No vibrational fine structure was included in the simulations, only 0−0 transitions were considered. Line widths of the Q_y and Soret bands of the simulated spectra were taken as experimental line widths in solution. The calculated vacuum spectra of bacterioclhorophylls were blue shifted with respect to the experimental solution spectra, especially in the Soret

TABLE 6: Excited States of Mg−Chlorin and Bacteriochlorophylls Bchl *c*, Bchl *d*, Bchl *e*, and Bchl *f* at PM3 Minimum Energy Obtained with the PM3 CISD (5,5) Method

state	main configuration (C ≥ |0.05|)
Mg−C Q_y	**0.44(H-1→L+1)** + 0.06(H-1→L+3) + **0.51(H→L)** − 0.06(H-3→L,H-1→L) + 0.08(H-1→L,H→L) −0.06(H-1→L+1,H→L+1) − 0.05(H-1→L+3,H→L+1) − 0.06(H→L,H→L+3)
Q_x	0.18(0) − 0.06(H-4→L) − **0.47(H-1→L)** + **0.45(H→L+1)** + 0.12(H-1,H→L,L+1) 0.07(H-1→L+1,H-1→L+1) + 0.08(H-1→L+1,H→L) + 0.07(H→L,H→L)
B	0.09(H-4→L+1) − 0.10(H-3→L) + 0.13(H-3→L+2) + **0.41(H-1→L+1)** − **0.19(H-1→L+3)** −**0.38(H→L)** + 0.06(H-3→L+1,H-1→L+1) + 0.09(H-3,H→L,L+1) + 0.06(H-3→L,H→L+1) −0.20(H-1→L,H-1→L+1) − 0.10(H-1,H→L+1,L+3) + 0.11(H-1→L,H→L) − 0.05(H-1→L,H→L+2) −0.09(H-1→L+3,H→L+1) − 0.09(H-1→L+3,H→L+1) − 0.08(H→L,H→L+1) + 0.05(H→L,H→L+3)
Bchl *c* Q_y	0.06(0) + 0.32(H-1→L+1) + 0.08(H-1→L+3) − **0.60(H→L)** − 0.05(H→L+2) − 0.07(H-1,H→L,L+1) − 0.06(H-1→L,H→L+1) − 0.05(H-1→L+1,H→L+1) + 0.05(H→L+1,H→L)
Q_x	−0.14(0) − **0.47(H-1→L)** + 0.08(H-1→L+1) − **0.42(H→L+1)** − 0.07(H→L+3) −0.06(H-1→L,H-1→L) + 0.18(H-1,H→L,L+1) + 0.09(H-1→L,H→L+1) 0.05(H-1→L,H→L+3) + 0.09(H-1→L+1,H→L) − 0.11(H→L,H→L)
B	0.23(H-2→L) − 0.08(H-1→L) − **0.21(H-1→L+1)** + **0.30(H-1→L+2)** - 0.06(H→L) −**0.50(H→L+2)** − 0.08(H→L+3) + 0.05(H-1→L,H-1→L+2) − 0.08(H-1→L+2,H-1→L+2) 0.06(H-1→L+2,H→L+2) + 0.05(H-1→L,H→L) + 0.05(H-1→L+2,H→L+1) 0.05(H-1,H→L,L+2) − 0.06(H→L+2,H→L+2)
Bchl *d* Q_y	0.06(0) + **0.32(H-1→L+1)** − 0.08(H-1→L+3) − **0.60(H→L)** + 0.05(H→L+2) + 0.07(H-1,H→L,L+1) 0.06(H-1→L,H→L+1) − 0.05(H-1→L+1,H→L+1) + 0.05(H→L+1,H→L)
Q_x	−0.14(0) − **0.46(H-1→L)** - 0.07(H-1→L+1) − **0.44(H→L+1)** + 0.07(H→L+3) −0.06(H-1→L,H-1→L) + 0.18(H-1,H→L,L+1) + 0.09(H-1→L,H→L+1) −0.05(H-1→L,H→L+3) + 0.09(H-1→L+1,H→L) − 0.11(H→L,H→L)
B	0.28(H-2→L) − 0.06(H-2→L+1) − 0.08(H-1→L) + **0.21(H-1→L+1)** − **0.27(H-1→L+2)** + 0.05(H→L) −**0.50(H→L+2)** + 0.08(H→L+3) + 0.05(H-2→L,H→L+1) − 0.07(H-1→L+2,H-1→L+2) 0.06(H-1→L+2,H→L+2) + 0.05(H-1,H→L,L+2) − 0.06(H→L+2,H→L+2)
Bchl *e* Q_y	0.05(H-2→L+1) + 0.10(H-1→L) + **0.35(H-1→L+1)** − 0.10(H-1→L+3) + **0.57(H→L)** −0.09(H→L+1) + 0.05(H→L+2) + 0.05(H→L+3) + 0.05(H-1,H→L,L+1) 0.06(H-1→L,H→L+1) − 0.05(H-1→L+1,H→L+1) − 0.05(H→L+1,H→L)
Q_x	−0.14(0) + **0.44(H-1→L)** - 0.13(H→L) − **0.44(H→L+1)** + 0.07(H→L+3) − 0.05(H-1→L,H-1→L) −0.19(H-1,H→L,L+1) + 0.05(H-1,H→L,L+3) − 0.10(H-1→L,H→L+1) 0.05(H-1→L,H→L+3) − 0.10(H-1→L+1,H→L) − 0.11(H→L,H→L)
B	0.14(H-2→L) − 0.05(H-1→L) + **0.25(H-1→L+1)** + **0.34(H-1→L+2)** + 0.06(H-1→L+3) −0.10(H→L) − **0.50(H→L+2)** − 0.09(H→L+3) − 0.05(H-1→L,H-1→L+2) −0.06(H-1→L+1,H→L) − 0.07(H-1→L+2,H→L+2) + 0.06(H→L+2,H→L+2)
Bchl *f* Q_y	0.05(H-2→L+1) + 0.09(H-1→L) + **0.35(H-1→L+1)** + 0.10(H-1→L+3) + **0.57(H→L)** −0.09(H→L+1) − 0.05(H→L+2) − 0.05(H-1,H→L,L+1) −0.06(H-1→L,H→L+1) −0.05(H-1→L+1,H→L+1)
Q_x	−0.14(0)- **0.43(H-1→L)** + 0.11(H→L) + **0.45(H→L+1)** + 0.08(H→L+3) −0.05(H-1→L,H-1→L) − 0.19(H-1,H→L,L+1) − 0.05(H-1,H→L,L+3) − 0.10(H-1→L,H→L+1) −0.05(H-1→L,H→L+3) − 0.10(H-1→L+1,H→L) − 0.11(H→L,H→L)
B	0.16(H-2→L) + **0.25(H-1→L+1)** − **0.32(H-1→L+2)** − 0.06(H-1→L+3) − 0.10(H→L) **0.50(H→L+2)** + 0.09(H→L+3) − 0.05(H-1→L,H-1→L+2) − 0.08(H-1→L+2,H-1→L+2) −0.05(H-1,H→L,L+2) − 0.06(H-1→L,H→L) − 0.07(H-1→L+2, H→L+2) − 0.05(H→L+2,H→L+2)

region (Figure 5). The Q_y transition energies of bacteriochlorins around 780 nm were predicted in increasing order, Bchl *h* < Bchl *b* < Bchl *a* < Bchl *g*, whereas for the corresponding transitions of chlorins around 650 nm, the corresponding order was Bchl *c* < Bchl *d* < Bchl *e* < Bchl *f*, in full accord with the experimental results (Table 7).[32,33] In Bchl *a*, Bchl *b*, and Bchl *g*, where the Q_x bands are clearly visible in the experimental spectra, the estimated Q_x transition energies were 10−20 nm off, independent of the method used.

3.4.2. Simulation of Spectra of 1:1 Complexes. In Figure 6, correlations between experimental and ZINDO/S CIS (20,20) transition energies of six Bchls with one acetone molecule coordinated to the central magnesium atom are shown. The results for Bchl *b* are given for diethyl ether. The experimental values in these calibrations were obtained from Gaussian fits of spectra recorded in acetone (Bchls *a*, *c*, *d*, *e*, and *g*) or in diethyl ether (Bchl *b*).[32,33] In chlorins where the assignment of the Q_x transition is not obvious, the most blue shifted resolved band component in the fitting region from 500 to 750 nm was used as representative of this transition (Table 8). In the Soret region, the wavelength of the red most major Gaussian component was used as a reference value.

Much improved correlations are obtained for 1:1 solvent complexes than for chromophores in a vacuum. Analysis of the CI coefficients of the complexes show that some solvent states are mixed with the chromophore states and the energy levels of the complexes are shifted with respect to the vacuum energies. The correlation between experimental and calculated transition energies of complexed Bchl *a* moves closer to the correlations of the "relative" choromophores Bchl *b* and *g*, an indication of stronger solvent interaction in Bchl *a* (Figure 6). The results are in very good agreement with the experimental transition energies recorded in acetone (Table 8).

Experimental solution spectra and simulated 1:1 acetone complex spectra of Bchls are shown in Figures 7 and 8. The results of Tables 7 and 8 show that solvent-induced shifts of the Q_y transitions of Bchl *a*, Bchl *b*, and Bchl *g* are small, whereas the shifts are more substantial for the Q_x bands, 20, 4, and 32 nm, respectively. In Bchl *c*, Bchl *d*, Bchl *e*, and Bchl *f*, only small solvent-induced spectral shifts of 5, 4, 4, and 1 nm of the Q_x transitions, respectively, were estimated. The agreement between the experimental and estimated Q_x transition energies in chlorins is fair. The energies are predicted 15−20 nm toward blue from the experimental values. This may be due to uncertainties of the assignments of the Q_x transitions (weak oscillator strengths) in the experimental spectra.

In the Soret region, calculated solvent-induced shifts for the red most major transitions for Bchl *a*, Bchl *b*, and Bchl *g* were

TABLE 7: Estimated Absorption Band Positions in a Vacuum (nm), Oscillator Strengths (*f*), and Experimental Band Positions[20] (nm) of Bacteriochlorophylls in Solution

molecule	Q_y (*f*) [nm]	Q_x (*f*) [nm]	Soret (*f*) [nm]
Bchl *a*	776 (0.6)	559 (0.0)	362 (0.4)
	775 (3.8)	562 (3.8)	361 (2.1)
	771 (0.8)	587 (0.1)	357 (1.8)
exp	773	577	358
Bchl *b*	796 (0.4)	583 (0.0)	385 (1.7)
	798 (3.7)	585 (4.3)	390 (2.6)
	785 (0.6)	608 (0.1)	386 (1.6)
exp	791	592	372
Bchl *c*	662 (0.4)	527 (0.1)	434 (1.7)
	664 (6.9)	608 (4.7)	440 (3.9)
	663 (0.6)	523 (0.0)	433 (3.0)
exp	659		429
Bchl *d*	653 (0.5)	519 (0.1)	425 (1.6)
	653 (7.1)	599 (4.8)	424 (3.4)
	655 (0.1)	516 (0.0)	428 (3.0)
exp	651		423
Bchl *e*	639 (0.4)	527 (0.2)	443 (1.8)
	630 (6.6)	585 (5.0)	426 (2.7)
	642 (0.5)	512 (0.1)	447 (2.7)
exp	647		458
Bchl *f*	630 (0.4)	520 (0.3)	432 (1.7)
	623 (6.9)	577 (5.0)	425 (1.8)
	637 (0.5)	506 (0.2)	441 (2.3)
exp			
Bchl *g*	763 (0.4)	540 (0.0)	380 (0.5), 374 (0.8)
	761 (3.8)	545 (4.6)	400 (2.8), 376 (2.0)
	763 (0.6)	576 (0.1)	393 (1.6), 358 (0.7)
exp	767	565	404, 364
Bchl *h*	835 (0.7)	580 (0.0)	335 (0.9)
	831 (5.0)	605 (4.2)	340 (1.9)
	828 (0.9)	618 (0.2)	344 (2.5)
exp			

[a] The first, second, and third row give the results of ZINDO/S CIS (15,15), PM3 CISD (5,5), and ab initio CIS(5,5)/6-31G* calculations of the transition energies, respectively.

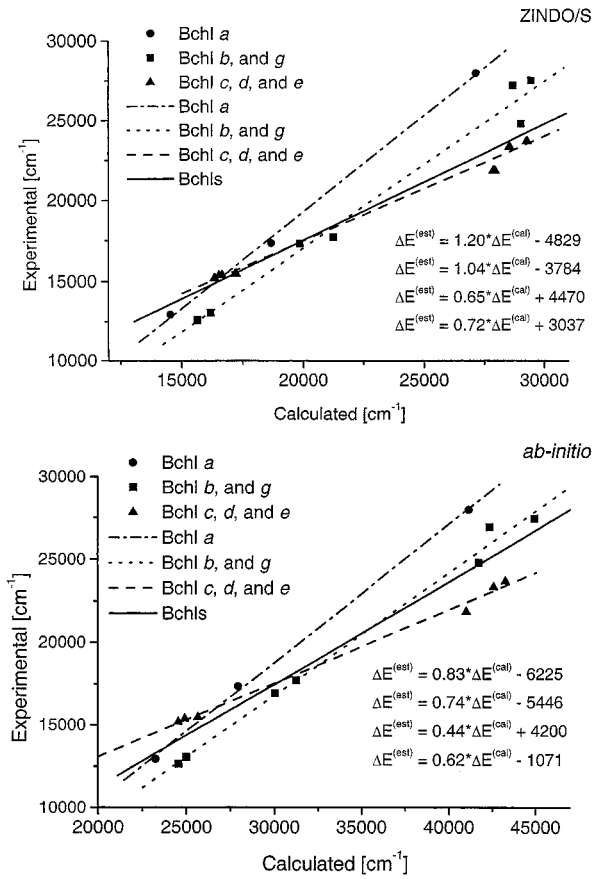

Figure 4. Linear correlations of the experimental (see Table 7) and computed Q_y, Q_x, and *B* (Soret) transition energies of bacteriochlorophylls in a vacuum (a) by using the ZINDO/S CIS (15,15) and (b) the ab initio (5,5)/6-31G* method, (dash dot) Bchl *a*; (dotted) Bchl *b* and Bchl *g*; (dashed) Bchl *c*, Bchl *d*, and Bchl *e*; and (solid) all bacteriochlorophylls. Equations from top to bottom: Bchl *a*; Bchl *b* and *g*; Bchl *c*, *d*, and *e*; and all Bchls.

33, 13, and 22 nm (Figure 7), and the corresponding values for Bchl *c*, Bchl *d*, Bchl *e*, and Bchl *f* were 6, 7, 12, and 9 nm (Figure 8), respectively. Simulated spectra of acetone−Bchl complexes in the Soret region have much more resemblance to the experimental solution spectra[22,56,57] than the corresponding vacuum spectra (Figure 5, 7, and 8). The solvent shifts in the Q_x and Soret regions reflect changes in the excited-state energies of the chromophores because of solvent coordination and the coefficients of the CI expansions. Such shifts for Bchl *a* and Bchl *e* are demostrated in Figure 5. The PM3 CISD method and ab initio CIS calculations failed to predict the oscillator strengths correctly (Table 8).

4. Discussion

The semiempirical PM3 calculations with full geometry optimization describe the experimental structure of the rings B and D of all bacterioclhorophylls very well, though it does not locate the magnesium atom exactly in the center of the porphyrin plane.[67,58] Such asymmetry effects have been reported earlier.[60] Despite this shortcoming, we think that the PM3 method may be used to calculate model structures of Bchls and Bchl-like molecules. For example, the method may be used to optimize structures of bacteriochlorophylls embedded in proteins by keeping the X-ray crystalline coordinates of the heavy atoms fixed and by adding the hydrogen atoms and minimizing the energy. Then spectroscopic transition energies and oscillator strengths may be calculated by using the ZINDO/S CI method.

The semiempirical PM3 method gives a positive charge of about +0.4 on the central magnesium atom of the Bchls. For the surrounding four nitrogen atoms, charges from 0.0 to +0.2 are obtained. Charges on oxygen atoms became all negative. Hartree−Fock ab initio calculations at the 6-31G* level for the PM3 minimum geometry give more realistic results: a positive atomic charge of about +1.3 on the magnesium atom, negative charges of about −1.0 on the nitrogen atoms, and negative charges on oxygen atoms ranging from −0.30 to −0.64 in all Bchls. The fact that the PM3 method does not predict atomic charges of magnesium and nitrogens of the porphyrin ring of chlorophylls[43] or bacteriochlorophylls correctly will limit the use the method in calculation of structures of large biological systems with nitrogen atoms present, e.g., DNA.

Ab initio 6-31G* charge distributions make noncovalent interactions possible where solvent molecules form 1:1 or 1:2 complexes with chlorophylls and bacteriochlorophylls in solution, suggested in several spectroscopic studies.[61−66] Self-aggregation of bacteriochlorophylls may occur via magnesium and oxygen atoms of the adjacent chromophores via electrostatic interactions. In particular, the $O13^1$ atom of bacteriochlorophylls may easily, without any steric hindrance, bind noncovalently to the positively charged Mg atom of the next bacteriochlorophyll forming a dimer or a larger aggregate.[67−78] Other negatively charged oxygen atoms, especially OR3, =OR7, OR7, and $=O13^2$ may have a role in aggregation processes.[79,80] Furthermore aggregates, where chlorophylls or bacteriochlrophylls are linked by solvent molecules may be formed in many ways with and without the oxygen atoms of the porphyrin ring being involved.[81−89]

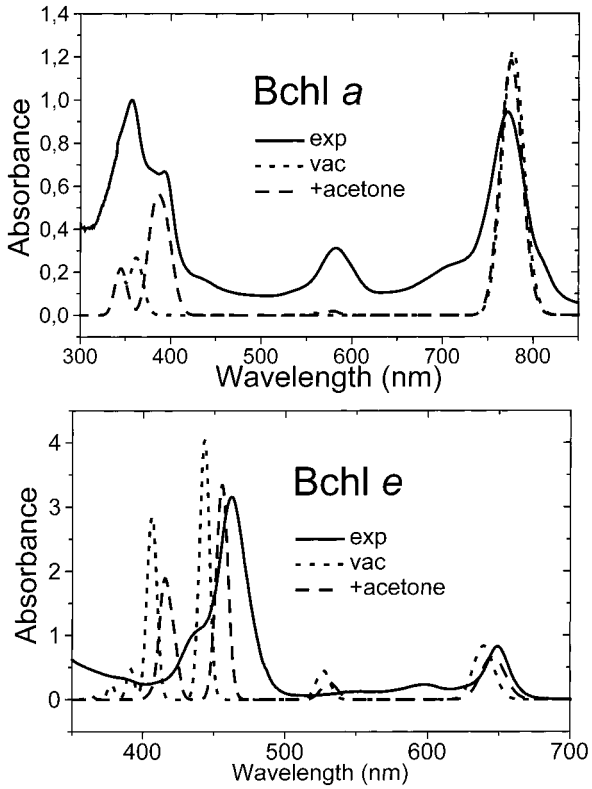

Figure 5. Experimental, simulated vacuum, and 1:1 acetone complex spectra of Bchl *a* and Bchl *e*. The ZINDO/S CIS (20,20) method and experimental line widths of the Q_y and Soret transitions and Gaussian line shape were used to simulate the spectra.

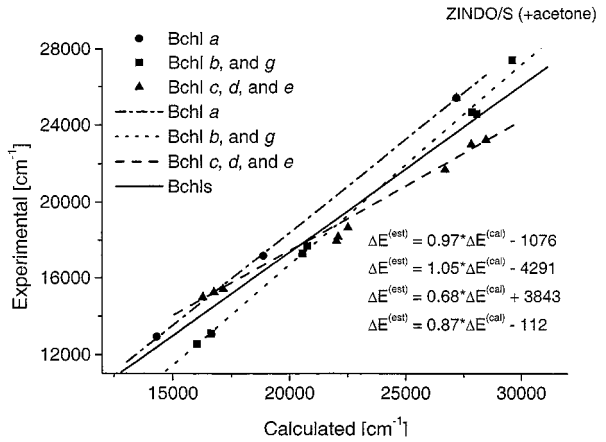

Figure 6. Linear correlations of Q_y, Q_x, and Soret transition energies of the bacteriochlorophylls forming 1:1 complex with acetone (see Table 8) obtained by using the ZINDO/S CIS (20,20) method, (dash dot) Bchl *a*; (dotted) Bchl *b* and Bch *g*; (dashed) Bchl *c*, Bchl *d*, and Bchl *e*; (solid) all bacteriochlorphylls. Equations from top to bottom: Bchl *a*; Bchl *b* and *g*; Bchl *c*, *d*, and *e*; all Bchls.

The excited states of the bacteriochlorophylls studied are linear combinations of pure configurations. Detailed examination of these configurations allows explaining the influence of solvent on excited state energies of bacteriochlorophylls. The number of main configurations increase as one goes from the lowest singlet excited state Q_y to the higher excited *B* states. Simultaneously the number and magnitude of pure configurations, which have nonzero amplitude on the Mg atom, increase. The states having amplitude on the Mg atom (Figure 3) are much more open to solvent interactions than the states with small amplitude on the Mg atom. Noncovalent interactions of a solvent molecule with the central Mg atom will produce small changes in electron densities of the ground and excited states of porphyrins and in the LCAO coefficients of MOs having amplitude on the Mg atom. This results in energetic shifts of the Q_x and *B* (Soret) states and solvent-induced spectral shifts.[54,55]

TABLE 8: Estimated (top row) Absorption Band Positions (nm) and Oscillator Strengths (*f*) and Experimental (bottom row) Band Positions (nm) of Bacteriochlorophylls in Acetone

molecule	Q_y (*f*) [nm]	Q_x (*f*) [nm]	Soret (*f*) [nm]
Bchl *a*	775 (0.6)	579 (0.0)	395 (0.4)
exp	773	583	394
Bchl *b*	798 (0.4)	579 (0.0)	398 (1.4)
exp	796	579	408
Bchl *c*	671 (0.4)	532 (0.1)	440 (1.6)
exp	667	557	436
Bchl *d*	657 (0.5)	523 (0.1)	432 (1.6)
exp	656	536	431
Bchl *e*	646 (0.4)	531 (0.2)	455 (1.8)
exp	649	550	462
Bchl *f*	638 (0.4)	521 (0.3)	443 (1.7)
exp			
Bchl *g*	760 (0.4)	572 (0.0)	402 (0.7), 375 (0.6)
exp	763	566	406, 366
Bchl *h*	833 (0.6)	609 (0.0)	381 (0.7)
exp			

[a] The ZINDO/S CIS(20,20) method was used for calculations and experimental transition energies of the Q_y, Q_x, and Soret bands are from acetone solutions.

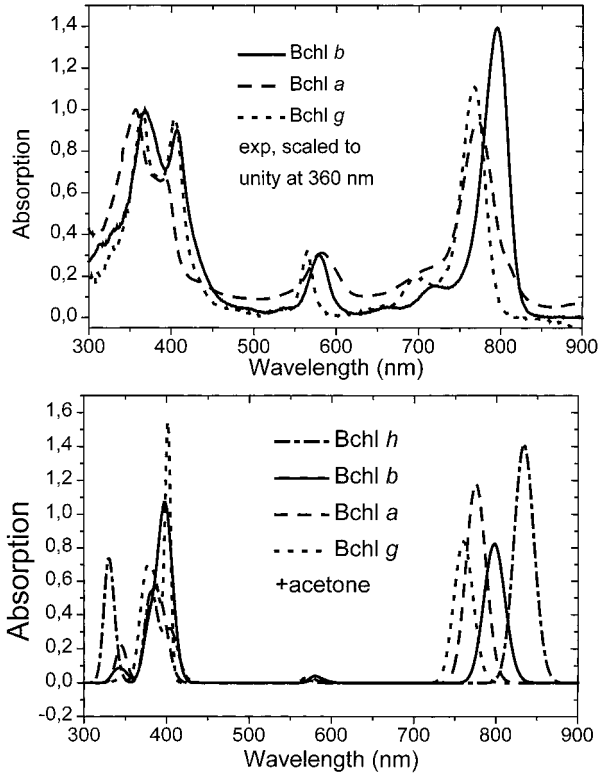

Figure 7. (a) Experimental and (b) simulated absorption spectra of Bchl *a*, Bchl *b*, Bchl *g*, and Bchl *h*. The experimental spectra have been recorded in acetone (Bchl *a*) and in ethyl ether (Bchl *b* and Bchl *g*). The experimental spectra of Bchl *b* and *g* were obtained from Dr. Christof Francke, University of Leiden. Simulated spectra were calculated for 1:1 acetone complexes. The method to simulate the spectra is the same as that in Figure 5.

Conclusions

We conclude by noting that the cost-effective ZINDO/S CIS (15,15) method may be used to describe spectroscopic properties

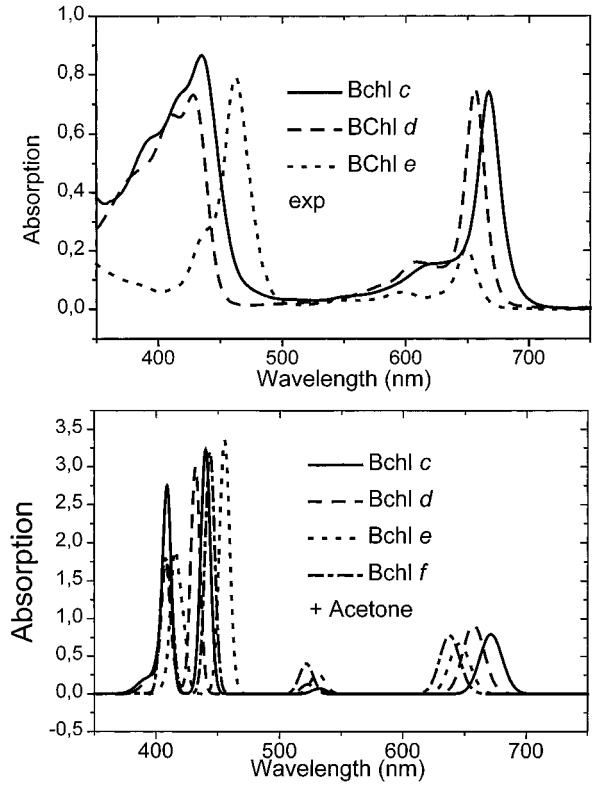

Figure 8. (a) Experimental and (b) simulated absorption spectra of Bchl *c*, Bchl *d*, Bchl *e*, and Bchl *f*. The experimental spectra have been recorded in acetone solution, and they were obtained from Dr. Carlos Borrego, University of Girona, Spain. Simulated spectra were calculated for 1:1 acetone complexes. The method to simulate the spectra is the same as that in Figure 5.

of bacteriochlorophylls. Linear correlations of experimental and calculated transition energies of the vacuum and 1:1 solvent complexes of Bchls were obtained, the latter approach giving better results. Such correlations are useful in evaluation of interaction energies and in predicting spectroscopic properties of chlorophylls and bacteriochlorophylls in solution, in aggregates or in protein environments, assuming that structural information of each environment is available.

The Q_y, Q_x, and Soret band positions and oscillator strengths of all Bchls studied could be correctly estimated. The exceptionally large red shift of the Soret band of Bchl *e* as compared to other chlorins came out nicely from the simulations. Spectra of not yet isolated hypothetical Bchls *f* and *h* were calculated for the first time. It was observed that the Q_x and Soret transitions are much more sensitive to solvent interactions than the Q_y transitions. This may be explained as a consequence of binding of a solvent molecule to the magnesium atom, that has high electron densities in the excited states giving rise to the Q_x and Soret transitions.

Acknowledgment. The authors acknowledge the financial support from the Academy of Finland (Contract Nos. 34192 and 44546) and computing resources from the Finnish National Centre of Scientific Computing, Espoo, Finland. Dr. Carles Borrego, Institute of Aquatic Ecology at the University of Girona and Dr. Cristof Francke, Department of Chemistry, Free University of Amsterdam, The Netherlands are acknowledged for sending us the solution spectra of Bchls in digital form. Professors Mette Miller (Odense), Thomas Gillbro (Umeå) and Jan Amesz (Leiden) are acknowledged for helpful discussions.

References and Notes

(1) Imhoff, J. F. In *Anoxygenic Photosynthetic Bacteria*; Blankenship, R. E., Madigan, M. T., Bauer, C. E., Eds.; Kluwer Academic Publishers: Dordrecht, The Netherlands, 1995; pp 1−15.

(2) Senge, O. M.; Schmith, K. M. In *Anoxygenic Photosynthetic Bacteria*; Blankenship, R. E., Madigan, M. T., Bauer, C. E., Eds.; Kluwer Academic Publishers: Dordrecht, The Netherlands, 1995; pp 137−149.

(3) Scheer, H. In *Chlorophylls*; Scheer, H., Ed.; CRC Press: Boca Raton, FL, 1991; pp 3−17.

(4) Madigan, M. T.; Ormerod, J. G. In *Anoxygenic Photosynthetic Bacteria*; Blankenship, R. E., Madigan, M. T., Bauer, C. E. Eds.; Kluwer Academic Publishers: Dordrecht, The Netherlands, 1995; pp 17−30.

(5) Thompson, M. A.; Fajer, J. *J. Phys. Chem.* **1992**, *96*, 2933.

(6) Chow, H.-C.; Serlin, R.; Strouse, C. E. *J. Am. Chem. Soc.* **1975**, *97*, 7230.

(7) Serlin, R.; Chow, H.-C.; Strouse, C. E. *J. Am. Chem. Soc.* **1975**, *97*, 7237.

(8) Kratsky, C.; Dunitz, J. D. *Acta Crystallogr. B* **1975**, *31*, 1586.

(9) Kratsky, C.; Dunitz, J. D. *Acta Crystallogr. B* **1977**, *33*, 545.

(10) Kratsky, C.; Isenring, H. P.; Dunitz, J. D. *Acta Crystallogr. B* **1977**, *33*, 547.

(11) Barkiga, K. M.; Gottfried, D. S. *Acta Crystallogr. C* **1994**, *50*, 2069.

(12) Barkiga, K. M.; Chantranupong, L.; Smith, K. M.; Fajer, J. *J. Am. Chem. Soc.* **1988**, *110*, 7566.

(13) Barkiga, K. M.; Fajer, J.; Chang, C. K.; Young, R. *J. Am. Chem. Soc.* **1984**, *106*, 6457.

(14) Barkiga, K. M.; Miura, M.; Thompson, M. A.; K. M.; Fajer, J. *Inorg. Chem.* **1991**, *30*, 2233.

(15) Miller, K. R. *Nature* **1982**, *300*, 53.

(16) Deisenhofer, J.; Epp, O.; Miki, R.; Huber, R.; Michel, H. *Nature* **1985**, *318*, 618.

(17) Chang, C. H.; Tiede, D.; Tang, J.; Smith, H.; Norris, J. R.; Schiffer, M. *FEBS Lett.* **1986**, *205*, 82.

(18) McDermott, G.; Prince, S. M.; Feer, A. A.; Hawthornthwaite-Lawless, A. M.; Papiz, M. Z.; Cogdell, R. J.; Isaacs, N. W. *Nature* **1995**, *374*, 517.

(19) Koepke, J.; Hu, X.; Muenke, C.; Schulten, K.; Michel, H. *Structure* **1996**, *4*, 581.

(20) Hoff, A. J.; Amesz, J. In *Chlorophylls*; Scheer, H., Ed.; CRC Press: Boca Raton, FL, 1991; pp 723−738.

(21) Dorough, G. D.; Miller, J. R. *J. Am. Chem. Soc.* **1952**, *74*, 6106.

(22) Bellacchio, E.; Sauer, K. *J. Phys. Chem.* **1999**, *103B*, 2279.

(23) Umetsu, M.; Wang, Z.-Y.; Kabayashi, M.; Nozawa, T. *Biochim. Biophys. Acta* **1999**, *1410*, 19.

(24) Planner, A.; Dudkowiak, A *J. Photochem. Photobiol.* **1998**, *115*, 151.

(25) Lapogue, K.; Näveke, A.; Gall, A.; Ivancich, A.; Seguin, J.; Scheer, H.; Strugis, J. N.; Mattioli, T. A.; Robert, B. *Biochemistry* **1999**, *38*, 11115.

(26) Nishizawa, E.; Hashimoto, H.; Koyama, Y. *Chem. Phys. Lett.* **1991**, *181*, 387.

(27) Thijssen, H. P. H.; Völker, S. *Chem. Phys. Lett.* **1981**, *82*, 478.

(28) Jeffrey, S. W. *Biochim. Biophys. Acta* **1969**, *177*, 456.

(29) Miller, M.; Gillbro, T.; Olson, J. M. *Photochem. Photobiol.* **1993**, *57*, 98.

(30) Steensgard, D. B.; Matsuura, K.; Cox, R. P.; Miller, M. *Photochem. Photobiol.* **1993**, *57*, 98.

(31) Frackowiak, D.; Dudkowiak, A.; Ptak, A.; Malak, H.; Gryczynski, I.; Zelent, B. *J. Photochem. Photobiol.* **1999**, *44B*, 231.

(32) The experimental absorption spectra of Bchl *b* and Bchl *g* were obtained from Dr. Christof Francke, former Ph.D. student of Prof. Jan Amez, Univeristy of Leiden, The Netherlands. The wavelengths given are from Gaussian fits of the spectra in the Q_y, Q_x, and Soret regions.

(33) The experimental absorption spectra of Bchl *c*, Bchl *d*, and Bchl *e* in acetone were obtained from Dr. Carles Borrego, Institute of Aquatic Ecology, University of Girona, Spain. The wavelengths given are from Gaussian fits of the spectra in the Q_y, Q_x, and Soret regions.

(34) Borrego, C. M.; Arellano, J. B.; Abella, C. A.; Gillbro, T.; Garcia-Gil, J. *Photosynth. Res.* **1999**, *60*, 257.

(35) Linnanto, J.; Korppi-Tommola, J. E. I.; Helenius, V. M. *J. Phys. Chem.* **1999**, *103B*, 8739.

(36) Linnanto, J.; Korppi-Tommola, J. E. I. *J. Chin. Chem. Soc.* **2000**, *47*, 657.

(37) Hasegawa, J.; Ozeki, Y.; Ohkawa, K.; Hada, M.; Nakatsuji, H. *J. Phys. Chem.* **1998**, *102B*, 1320.

(38) Ghosh, A. *J. Phys. Chem.* **1997**, *101B*, 3290.

(39) Facelli, J. C. *J. Phys. Chem.* **1997**, *102B*, 2111.

(40) Marchi, M.; Hutter, J.; Parrinello, M. *J. Am. Chem. Soc.* **1996**, *118*, 7847.

(41) Zhang, L. Y.; Friesner, R. A. *J. Phys. Chem.* **1995**, *99*, 16479.

(42) Hanson, L. K.; Fajer, J.; Thompson, M. A.; Zerner, M. C. *J. Am. Chem. Soc.* **1987**, *109*, 4728.

(43) Linnanto, J.; Korppi-Tommola, J. E. I. *Phys. Chem. Chem. Phys.* **2000**, *2*, 4962.
(44) Stewart, J. J. P. *J. Comput. Chem.* **1989**, *10*, 209.
(45) *SPARTAN*, version 5.0, revision A; Wavefunction Inc.: Irvine, CA, 1993, 1994.
(46) Stewart, J. J. P. *QCPE Bull.* **1985**, *5*, 133.
(47) Ridley, J. E.; Zerner, M. C. *Theor. Chim. Acta (Berl.)* **1973**, *32*, 111.
(48) Ridley, J. E.; Zerner, M. C. *Theor. Chim. Acta (Berl.)* **1976**, *42*, 223.
(49) Zerner, M. C.; Loew, G. H.; Kirchner, R. F.; Mueller-Westerhoff, U. T. *J. Am. Chem. Soc.* **1980**, *102*, 589.
(50) *HyperChem Computational Chemistry*, *Part 2*: *Theory and Methods*; Hypercube, Inc.; Publication HC40-00-03-00.
(51) Frisch, M. J.; Trucks, G. W.; Schlegel, H. B.; Gill, P. M. W.; Johnson, B. G.; Robb, M. A.; Cheeseman, J. R.; Keith, T.; Petersson, G. A.; Montgomery, J. A.; Raghavachari, K.; Al-Laham, M. A.; Zakrzewski, V. G.; Ortiz, J. V.; Foresman, J. B.; Cioslowski, J.; Stefanov, B. B.; Nanayakkara, A.; Challacombe, M.; Peng, C. Y.; Ayala, P. Y.; Chen, W.; Wong, M. W.; Andres, J. L.; Replogle, E. S.; Gomperts, R.; Martin, R. L.; Fox, D. J.; Binkley, J. S.; Defrees, D. J.; Baker, J.; Stewart, J. P.; Head-Gordon, M.; Gonzalez, C.; Pople J. A. *Gaussian 94*, revision B.1; Gaussian Inc.: Pittsburgh, PA, 1995
(52) Pilar, F. L. *Elementary Quantum Chemistry*; McGraw-Hill: New York, 1990; p 300.
(53) Petke, J. D.; Maggiora, G. M.; Shipman, L. L.; Christoffersen, R. E. *J. Mol. Spectrosc.* **1978**, *71*, 64.
(54) Petke, J. D.; Maggiora, G. M.; Shipman, L. L.; Christoffersen, R. E. *J. Mol. Spectrosc.* **1978**, *73*, 311.
(55) Seely, G. R.; Jensen, R. G. *Spectrochim. Acta* **1965**, *21***,** 1835.
(56) Umetsu, M.; Wang, Z.-Y.; Kobayashi, M.; Nozawa, T. *Biochim. Biophys. Acta* **1999**, *1410*, 19.
(57) Seely, G. R.; Jensen, R. G. *Spectrochim. Acta* **1965**, *21*, 1835.
(58) Serlin, R.; Chow, H.-C.; Strouse, C. E. *J. Am. Chem. Soc.* **1975**, *97*, 7230.
(59) Stewart, J. J. P. *J. Comput. Chem.* **1991**, *12*, 320.
(60) Katz, J. J.; Closs, G. L.; Pennington, F. C.; Thomas, M. R.; Strain, H. H. *J. Am. Chem. Soc.* **1963**, *85*, 3801.
(61) Boxer, S. G.; Closs, G. L.; Katz, J. J. *J. Am. Chem. Soc.* **1974**, *96*, 7058.
(62) Renge, I.; Avarmaa, R. *Photochem. Photobiol.* **1985**, *42*, 253.
(63) Fujiwara, M.; Tasumi, M. *J. Phys. Chem.* **1986**, *90*, 250.
(64) Koyama, Y.; Umemoto, Y.; Akamatsu, A.; Uehara, K.; Tanaka, M. *J. Mol. Struct.* **1986**, *146*, 273.
(65) Sato, H.; Okada, K.; Uehara, K.; Ozaki, Y. *Photochem. Photobiol.* **1995**, *61*, 175.
(66) Closs, G. L.; Katz, J. J.; Pennington, F. C.; Thomas, M. R.; Strain, H. H. *J. Am. Chem. Soc.* **1963**, *85*, 3809.
(67) Sauer, K.; Smith, J. R. L.; Schultz, A. J. *J. Am. Chem. Soc.* **1966**, *88*, 2681.
(68) Ballschmiter, K.; Katz, J. J. *J. Am. Chem. Soc.* **1969**, *91*, 2661.
(69) Ballschmiter, K.; Truesdell, K.; Katz, J. J. *Biochim. Biophys. Acta* **1969**, *184*, 604.
(70) Katz, J. J.; Janson, T. R.; Kostka, A. G.; Uphaus, R. A. *J. Am. Chem. Soc.* **1972**, *94*, 2883.
(71) Trifunac, A. D.; Katz, J. J. *J. Am. Chem. Soc.* **1974**, *96*, 5233.
(72) Hynninen, P. H. *Z. Naturforsch.* **1984**, *39B*, 675.
(73) Kooyman, R. P. H.; Schaafsma, T. J. *J. Am. Chem. Soc.* **1984**, *106*, 551.
(74) Abraham, R. J.; Goff, D. A.; Smith, K. M. *J. Chem. Soc., Perkin Trans.* **1988**, *1*, 2443.
(75) Thibodeau, D. L.; Koningstein, J. A. *J. Phys. Chem.* **1989**, *93*, 7713.
(76) Hynninen, P. H.; Lötjönen, S. *Biochim. Biophys. Acta* **1993**, *1183*, 381.
(77) Oba, T.; Furukawa, H.; Wang, Z.-Y.; Nozawa, T.; Mimuro, M.; Tamiaki, H.; Watanabe, T. *J. Phys. Chem. B* **1998**, *102*, 7882.
(78) Fong, F. K.; Koester, V. J. *J. Am. Chem. Soc.* **1975**, *97*, 6888.
(79) Abraham, R. J.; Smith, K. M. *J. Am. Chem. Soc.* **1983**, *105*, 5734.
(80) Katz, J. J.; Ballschmiter, K.; Garcia-Morin, M.; Strain, H. H.; Uphaus, R. A. *Proc. Natl. Acad. Sci. U.S.A.* **1968**, *60*, 100.
(81) Le Brech, J.; Leblanc, R. M.; Antippa, A. F. *Chem. Phys. Lett.* **1974**, *26*, 37.
(82) Fong, F. K. *Proc. Natl. Acad. Sci. U.S.A.* **1974**, *71*, 3692.
(83) Fong, F. K. *J. Am. Chem. Soc.* **1975**, *97*, 6890.
(84) Shipman, L. L.; Cotton, T. M.; Norris, J. R.; Katz, J. J. *Proc. Natl. Acad. Sci. U.S.A.* **1976**, *73*, 1791.
(85) Fong, F. K.; Koester, V. J.; Polles, J. S. *J. Am. Chem. Soc.* **1976**, *98*, 6407.
(86) Gurinovich, G. P.; Zenkevich, E. I.; Chirvony, V. S.; Gadonas, R.; Pelakauskas, A. *Exp. Technol. Phys.* **1989**, *37*, 335.
(87) Uehara, K.; Mimuro, M.; Tanaka, M. *Photochem. Photobiol.* **1991**, *53*, 371.
(88) Oksanen, J. A. I.; Helenius, V. M.; Hynninen, P. H.; van Amerongen, H.; Korppi-Tommola, J. E. I.; van Grondelle, R. *Photochem. Photobiol.* **1996**, *64*, 356.
(89) Oba, T.; Mimuro, M.; Wang, Z.-Y.; Nozawa, T.; Yoshida, S.; Watanabe, T. *J. Phys. Chem. B* **1997**, *101*, 3261.